

## Supplementary Information

# Temperature-dependent interfacial reactions between sulfide argyrodite solid electrolyte and lithium metal anode

*Ye-Eun Park,<sup>a</sup> SeoungJae Kang,<sup>a</sup> Taehyun Kim,<sup>a</sup> Huijeong Oh,<sup>a</sup> Kyungsu Kim,<sup>b</sup> Woosuk Cho,<sup>b</sup> and  
Sangryun Kim<sup>\*a, c</sup>*

<sup>a</sup>Department of Chemistry, Gwangju Institute of Science and Technology (GIST), 123 Cheomdangwagi-ro, Buk-gu, Gwangju, 61005, Republic of Korea.

<sup>b</sup>Advanced Batteries Research Center, Korea Electronics Technology Institute (KETI), 25 Saenari-ro, Seongnam 13509, Republic of Korea.

<sup>c</sup>Graduate School of Energy Convergence, Gwangju Institute of Science and Technology (GIST), 123 Cheomdangwagi-ro, Buk-gu, Gwangju, 61005, Republic of Korea.

\*Corresponding author

E-mail address: sangryun@gist.ac.kr

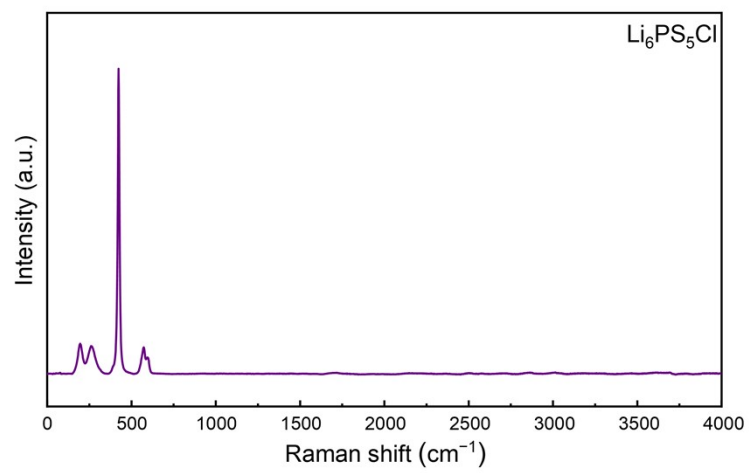


**Fig. S1** Raman spectra of  $\text{Li}_6\text{PS}_5\text{Cl}$ .

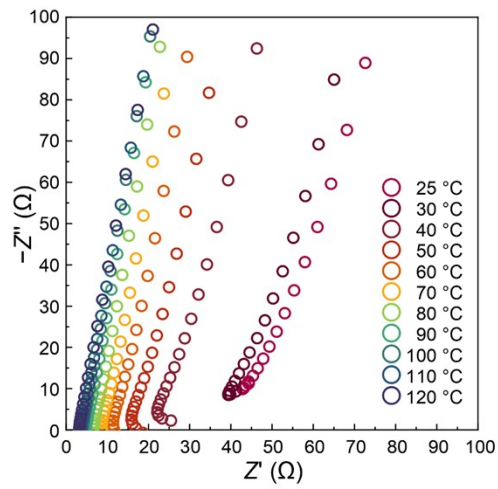


**Fig. S2** Nyquist plots of Au/Au blocking cells over the temperature range of 25 °C to 120 °C. The impedance was determined by the  $x$ -axis intercept of the single spike.<sup>1,2</sup>

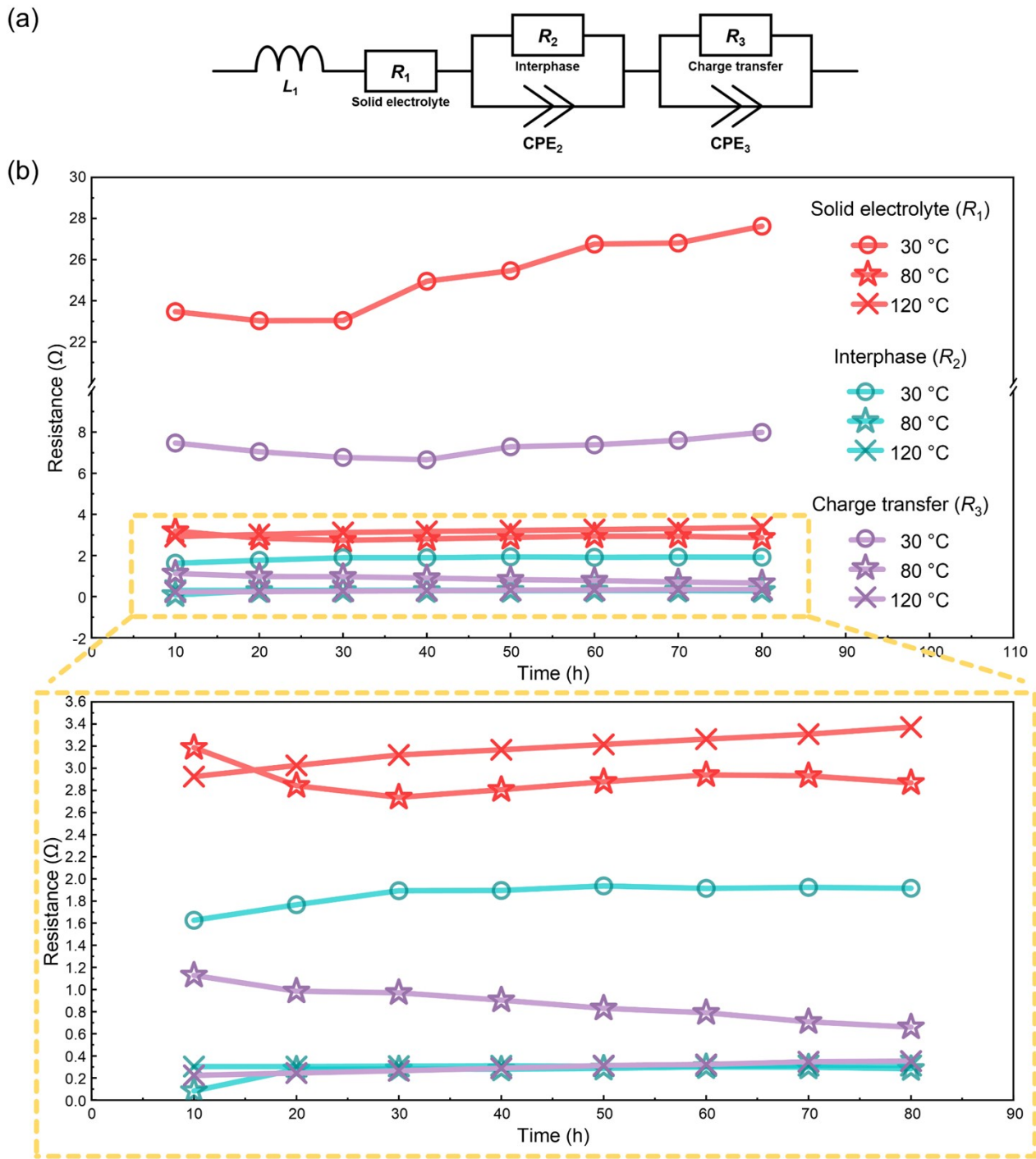


**Fig. S3** (a) Equivalent circuit model used to fit the EIS data obtained at 30, 80 and 120 °C. (b) Temperature-dependent evolution of impedance fitting parameters. In the low-frequency region, Nyquist plots did not exhibit a complete semicircle due to the presence of an inductive loop.<sup>3</sup> Therefore, the trailing region was excluded from the fitting.

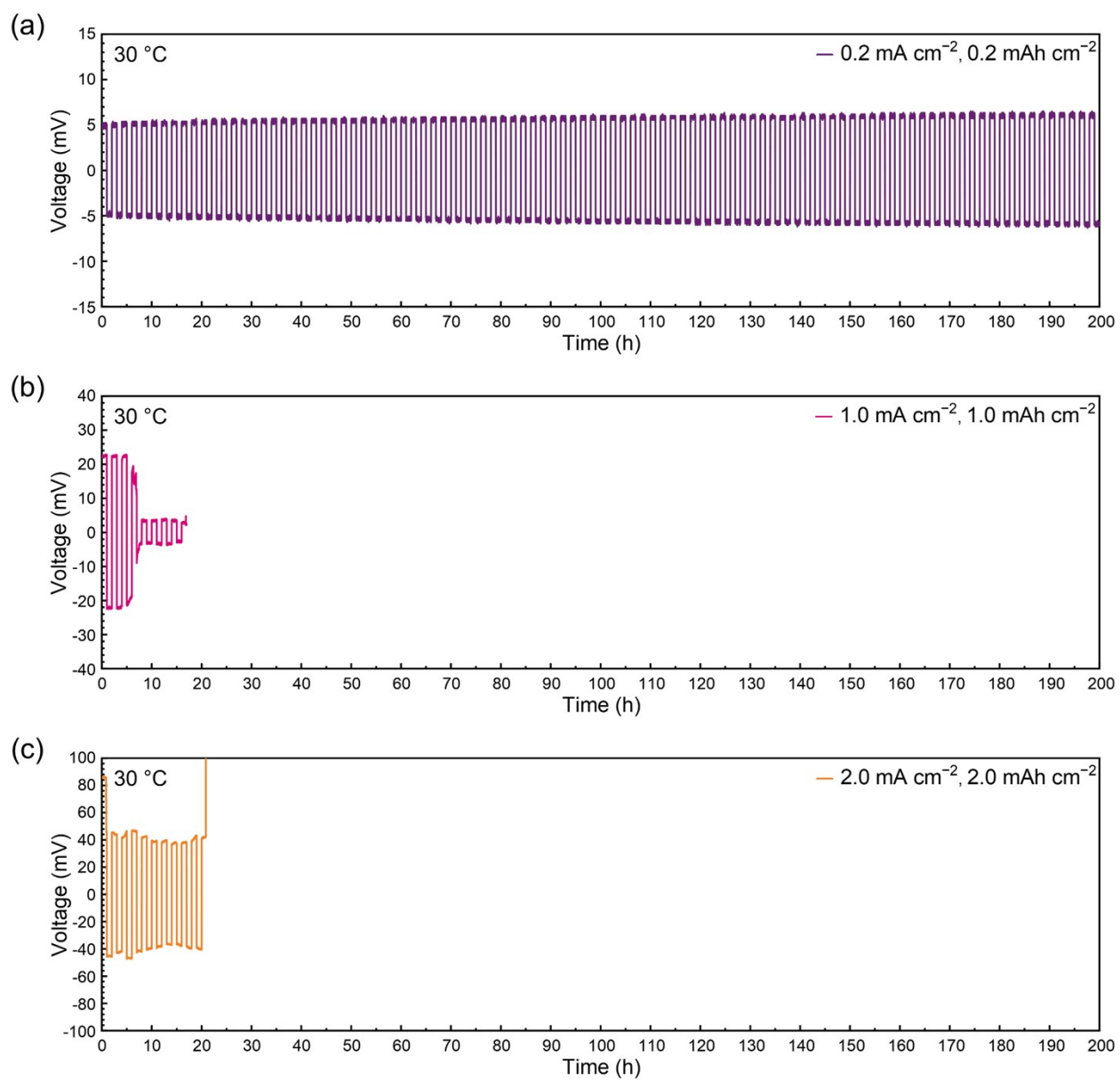


**Fig. S4** Galvanostatic Li stripping and plating cycling profiles measured under various current densities of (a) 0.2, (b) 1, and (c) 2 mA cm<sup>-2</sup> at 30 °C.

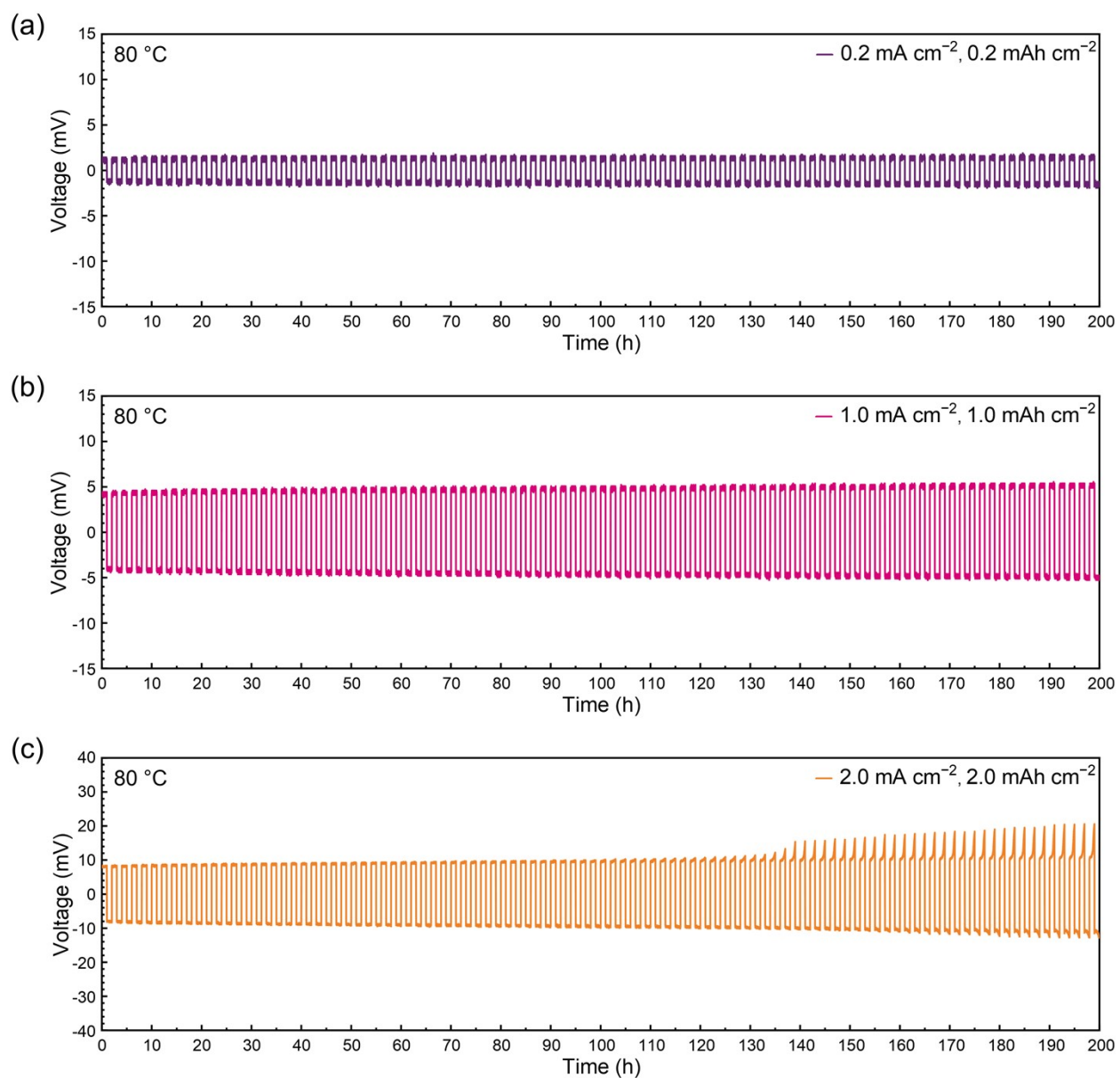


**Fig. S5** Galvanostatic Li stripping and plating cycling profiles measured under various current densities of (a) 0.2, (b) 1, and (c) 2 mA cm<sup>-2</sup> at 80 °C.

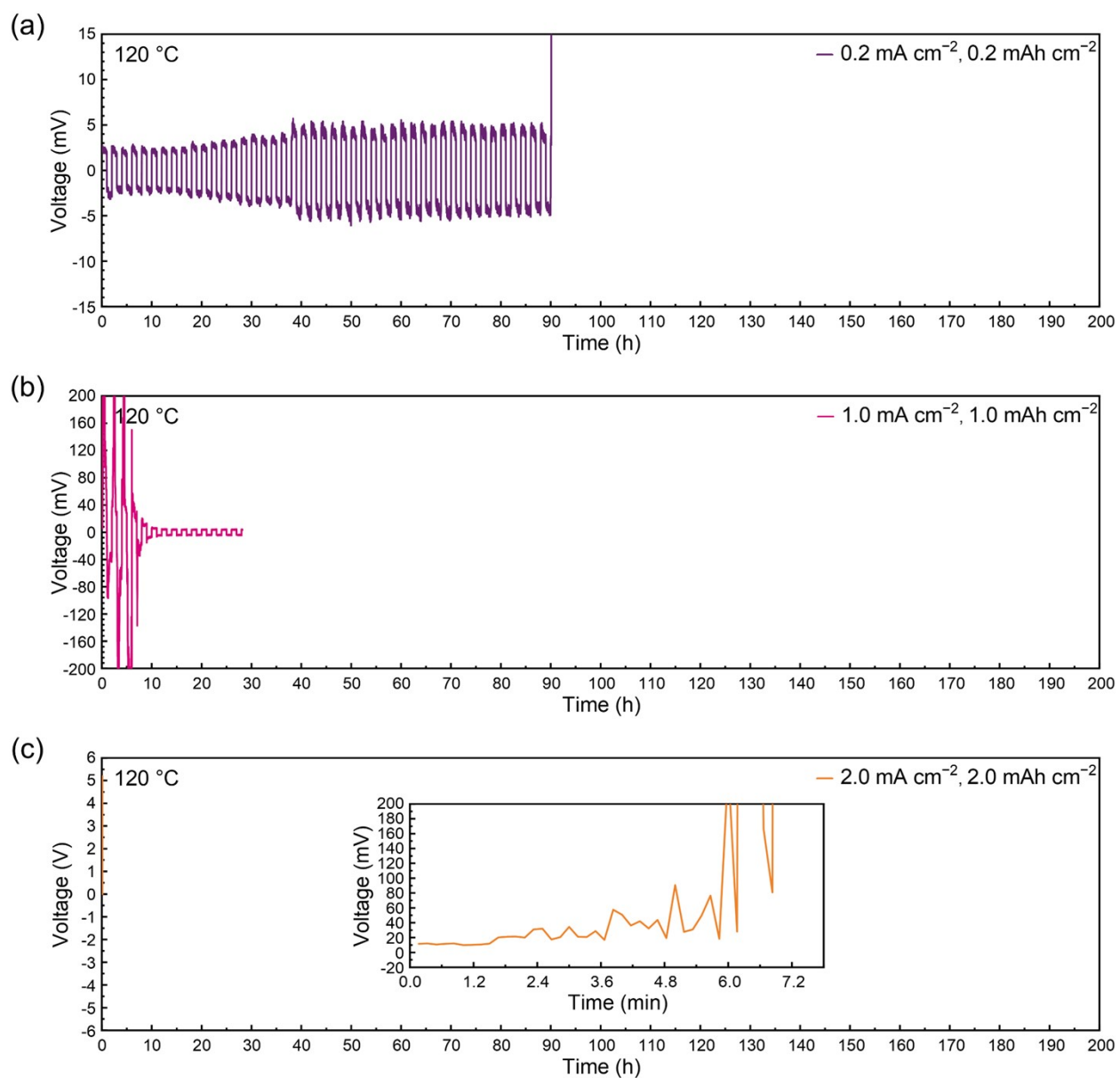


**Fig. S6** Galvanostatic Li stripping and plating cycling profiles measured under various current densities of (a) 0.2, (b) 1, and (c) 2 mA cm<sup>-2</sup> at 120 °C. The inset of Fig. S5c shows a magnified view of the initial cycling region.

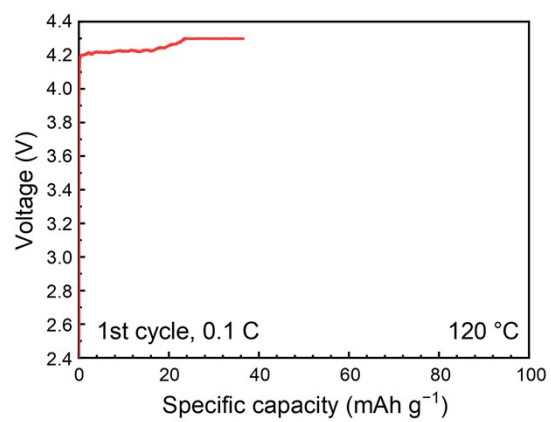


**Fig. S7** The first charge profile of the  $\text{LiNi}_{0.9}\text{Co}_{0.05}\text{Mn}_{0.05}\text{O}_2/\text{Li}_6\text{PS}_5\text{Cl}/\text{Li}$  cell at 0.1C and 120 °C.

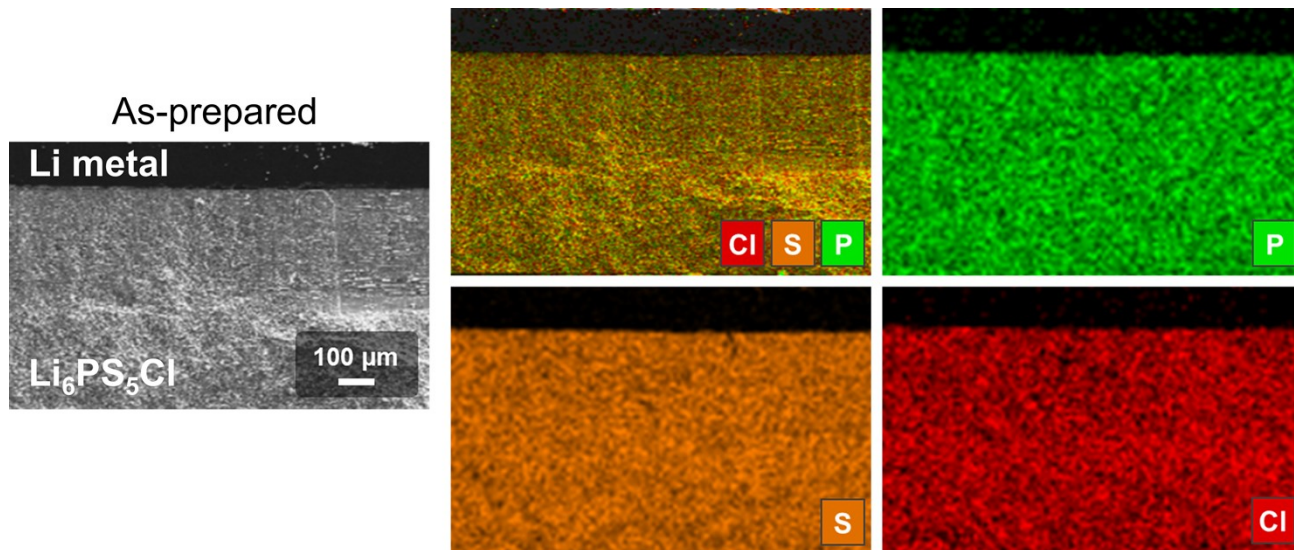


**Fig. S8** Cross-sectional SEM image and EDX elemental mapping of P, S, and Cl for the as-prepared Li/Li<sub>6</sub>PS<sub>5</sub>Cl interface before Li plating/stripping reactions.

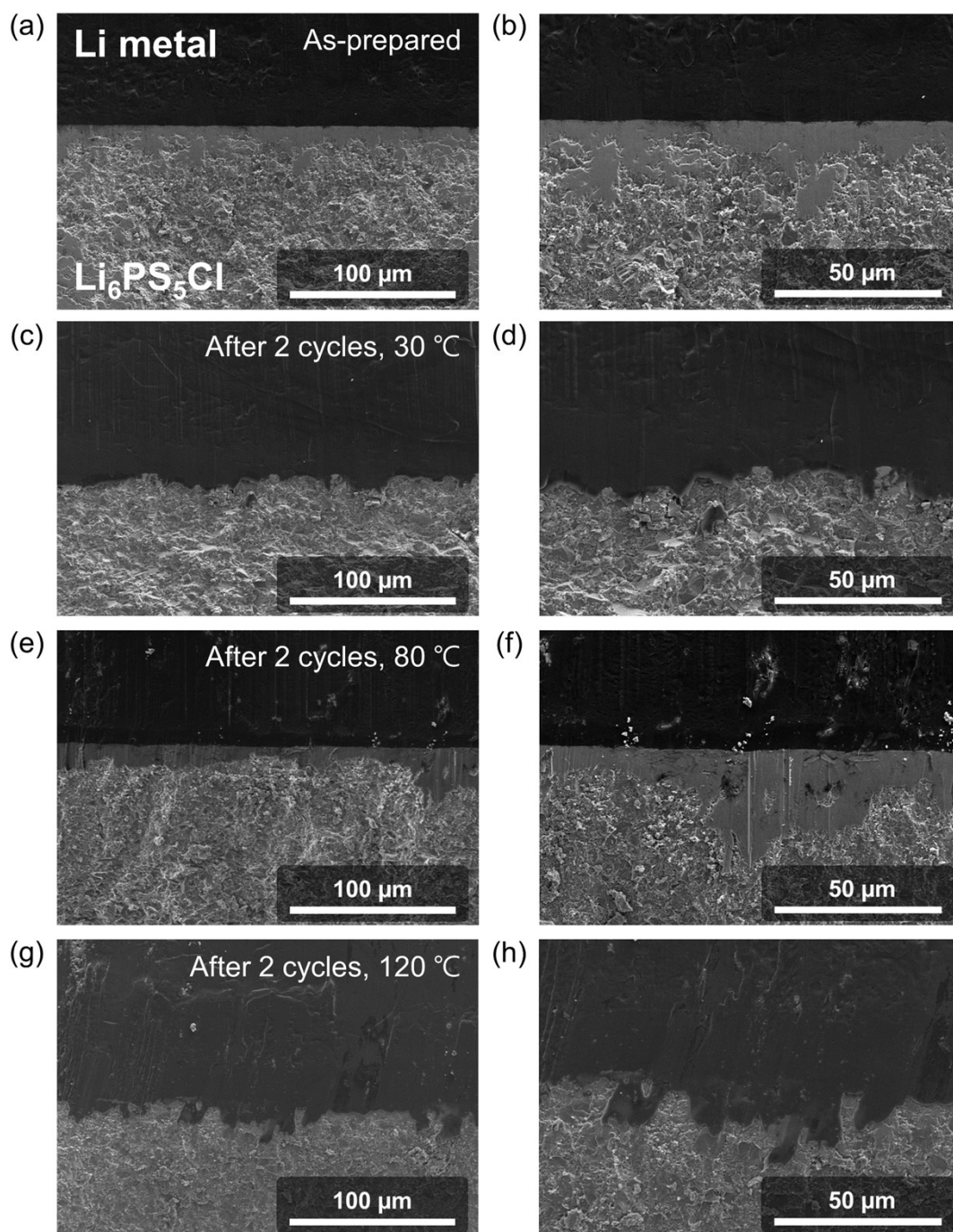


**Fig. S9** Cross-sectional SEM images of the Li/Li<sub>6</sub>PS<sub>5</sub>Cl interface (a, b) before and after Li plating/stripping reactions at (c, d) 30, (e, f) 80, and (g, h) 120 °C. The measurements were conducted after two cycles at a current density of 0.2 mA cm<sup>-2</sup> in multiple measurement regions.

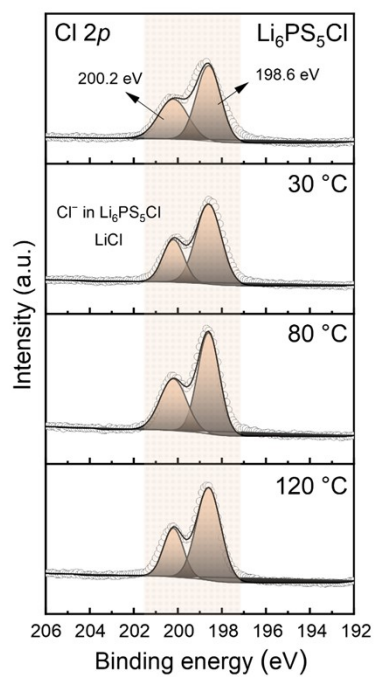


**Fig. S10** XPS spectrum of Cl  $2p$  for the Li/ $\text{Li}_6\text{PS}_5\text{Cl}$  interface. The measurements were conducted after 20-hour reactions of  $\text{Li}_6\text{PS}_5\text{Cl}$  with Li metal at 30, 80, and 120 °C.

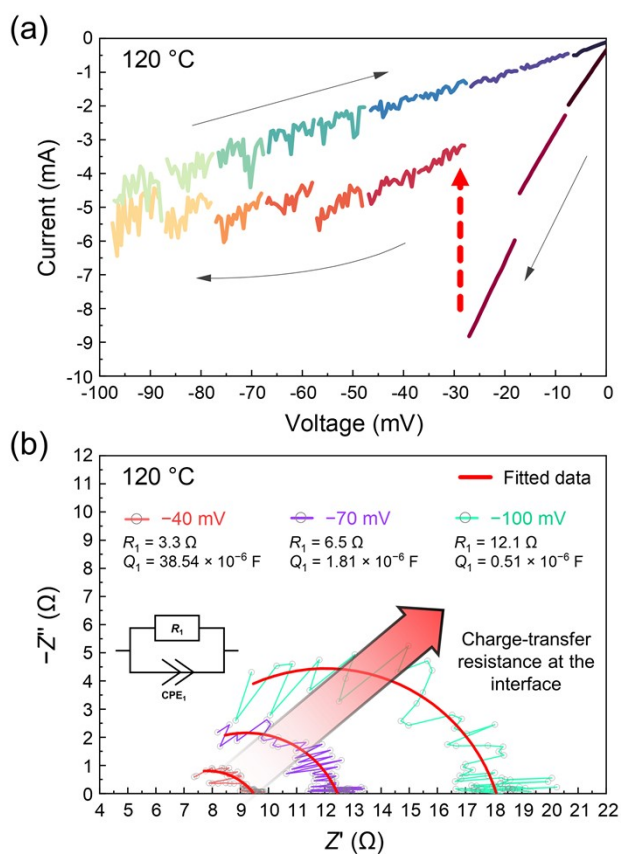


**Fig. S11** (a) CV results at a scan rate of 0.1 mV s<sup>-1</sup> using a Li/Li<sub>6</sub>PS<sub>5</sub>Cl/Li symmetric cell at 120 °C, measured every 10 mV. (b) *In-situ* EIS spectra measured at selected potentials (-40, -70, and -100 mV) during the CV test in Fig. S11a, along with the fitted curves using an equivalent circuit consisting of one parallel combination of a constant phase element (CPE) and a resistor.

## REFERENCES

1. B.-A. Mei, J. Lau, T. Lin, S. H. Tolbert, B. S. Dunn and L. Pilon, Physical Interpretations of Electrochemical Impedance Spectroscopy of Redox Active Electrodes for Electrical Energy Storage, *J. Phys. Chem. C*, 2018, **122**, 24499–24511.
2. H. Kim, T. Kim, S. Joo, J. Kim, J. Noh, J. Ma, J.-J. Woo, S. Choi, K. Kim, W. Cho, K. Kisu, S. Orimo and S. Kim, Aqueous synthesis of lithium superionic-conducting complex hydride solid electrolytes, *J. Mater. Chem. A*, 2024, **12**, 32132–32139.
3. Z. Tan, Z. Wang, S. Zhang, S. Bai, D. Zhang, Y. Jin and S. Xing, Corrosion behavior of X80 pipeline steel local defect pits under static liquid film, *Sci. Rep.*, 2021, **11**, 20755.